BlotGlycoABC™, an Integrated Glycoblotting Technique for Rapid and Large Scale Clinical Glycomics*[S]

Yoshiaki Miura‡, Megumi Hato‡, Yasuro Shinohara‡, Hiromitsu Kuramoto§, Jun-ichi Furukawa‡, Masaki Kurogochi‡, Hideyuki Shimaoka§, Mitsuhiro Tada¶, Kazuaki Nakanishi‖, Michitaka Ozaki‖, Satoru Todo‖, and Shin-Ichiro Nishimura‡****

Recent progress in mass spectrometry has led to new challenges in glycomics, including the development of rapid glycan enrichment techniques. A facile technique for exploration of a carbohydrate-related biomarker is important because proteomics research targets glycosylation, a posttranslational modification. Here we report an "all-in-one" protocol for high throughput clinical glycomics. This new technique integrates glycoblotting-based glycan enrichment onto the BlotGlycoABC™ bead, on-bead stabilization of sialic acids, and fluorescent labeling of oligosaccharides in a single workflow on a multiwell filter plate. The advantage of this protocol and MALDI-TOF MS was demonstrated through differentiation of serum *N*-glycan profiles of subjects with congenital disorders of glycosylation and hepatocellular carcinoma and healthy donors. The method also permitted total cellular glycomics analysis of human prostate cancer cells and normal human prostate epithelial cells. These results demonstrate the potentials of glycan enrichment/processing for biomarker discovery. ***Molecular & Cellular Proteomics 7:370–377, 2008.***

Large scale and quantitative glycomics is an important and promising approach because the difference in glycan expression between disease and healthy states is expected to be a useful tool for the diagnosis or prognosis of diseases (1). Mass spectrometric methods are now exclusively applied for the structural analysis and sequencing study of carbohydrates (2, 3). Due to the notable improvements in MS technology including methods of ionization, fragmentation, and detection (4–6), MS is preferred to other analytical methods, such as HPLC and nuclear magnetic resonance spectroscopy, in glycomics. In particular, MALDI-TOF and ESI MS that deliver mild ionization of glycans and high throughput analysis are potential candidates for primary techniques.

However, there is no PCR-like glycan amplification technology for glycomics because glycan biosynthetic process is not template-driven and is subject to multiple sequential and competitive enzymatic steps. Although partial peptide fragments detected in proteomics are fully supported by full-length protein/DNA sequence databases, glycomics requires the enrichment of total glycans from highly complicated mixtures such as serum, cells, and tissues. Therefore, one crucial bottleneck in structural and functional glycomics is the tedious and time-consuming multistep process for the purification of trace amounts of glycans. For example, glycans, once released from glycoproteins or glycolipids, are often subjected to fluorescent labeling and purification for detection in HPLC analysis (7, 8). In addition, oligosaccharides containing sialic acids are further modified to stabilize or enhance the sensitivity of anionic glycans in MS measurement (9–11). In some cases, sialic acids are deleted for the simplification or limitation of detection even though important information will be lost. Recently a DNA sequencer has also been utilized for clinical *N*-glycan profiling (12, 13) in which the above mentioned multistep procedures of purification and derivatization suited for capillary electrophoresis are still required. In general, protocols for the preparation of glycan derivatives vary depending upon the analytical methods and require specialized expertise for step-by-step handling. These technical but crucial problems in the enrichment of glycans make it impossible to achieve reliable and high throughput glycomics (14).

Our recent efforts have been directed to the establishment of practical methods for glycan enrichment, namely "*glycoblotting*" (15–20). The optimized protocol requires only 5 μl of human serum for the quantitative profiling of 30–40 kinds of major glycoforms within 5–8 h (19). These attempts clearly indicated the advantage of incorporation of solid support in the facile and efficient manipulation of enriched glycans, yielding higher recovery and reducing complicated operations. We present herein an "all-in-one" solution for automated and high throughput *N*-glycan enrichment and processing that is greatly beneficial in "real world" clinical glycomics. This system permits the integration of multiple

From the ‡Graduate School of Life Science and Frontier Research Center for Post-Genomic Science and Technology, Hokkaido University, Sapporo 001-0021, Japan, §Sumitomo Bakelite Co., Kobe 651-2241, Japan, ¶Division of Cancer-Related Genes, Institute for Genetic Medicine, Hokkaido University, Sapporo 060-0815, Japan, and ‖Department of General Surgery, Graduate School of Medicine, Hokkaido University, Sapporo 060-8638, Japan

Received, August 13, 2007, and in revised form, October 25, 2007
Published, MCP Papers in Press, November 5, 2007, DOI 10.1074/mcp.M700377-MCP200

steps such as selective capturing of total glycans, methyl esterification of sialic acids, and fluorescent tagging in a single workflow based on the combined use of a hydrazide-functionalized bead with multiwell filter plate handling. We believe that this *de facto* standardized technology will allow for large scale clinical glycomics/glycoproteomics and accelerate the discovery of new disease-related biomarkers.

EXPERIMENTAL PROCEDURES

Materials

The clinical study was approved by the local ethics committee of Hokkaido University Hospital. Informed consent was obtained from all serum donors. Peptide-*N*-glycosidase F (PNGase F)[1] was purchased from Roche Applied Science. 3-Methyl-1-*p*-tolyltriazene, 8 M borane-pyridine complex, and DTT were from Sigma-Aldrich. BlotGlycoABC™ was prepared as described in the supplemental note and is now commercially available from Sumitomo Bakelite, Co., Tokyo, Japan. Other reagents and solvents were obtained from Wako Pure Chemicals Co., Tokyo, Japan, unless otherwise stated. Sera of congenital disorders of glycosylation (CDG) patients were kindly provided by Prof. H. H. Freeze, Burnham Institute for Medical Research, La Jolla, CA.

Release of N-Glycans from Human Serum

Whole human serum was treated according to the condition reported previously (20) by our group to release reducing *N*-glycans. Briefly a 10-μl aliquot of serum was diluted 6-fold in 83 mM ammonium bicarbonate containing a detergent and 10 mM DTT. After incubation for 30 min at 60 °C, 1 volume (10 μl) of 123 mM iodoacetamide was added, and the mixture was incubated for an hour at room temperature in the dark. To the solution was added 400 units of trypsin (Sigma-Aldrich), and the mixture was incubated for an hour at 37 °C. After heat inactivation of trypsin, 2 units of PNGase F were added to the mixture, and the sample was incubated at 37 °C overnight. The released total (neutral and sialyl) *N*-glycans in a digest mixture were used directly for glycoblotting by means of the BlotGlycoABC bead.

General Protocol of Glycoblotting by BlotGlycoABC

40 μl of BlotGlycoABC beads (50% suspension) was aliquoted to a well of a filter plate (MultiScreen Solvinert, Millipore). The beads were washed with 1 M aqueous acetic acid (AcOH), 50% aqueous acetonitrile, and ACN successively using a vacuum manifold. 20 μl of whole serum sample digested with trypsin and PNGase F, equivalent to 2.5 μl of serum, was transferred to the well followed by the addition of 200 μl of 2% AcOH in acetonitrile. The plate was incubated at 80 °C to dryness in a TurboVap 96 concentrator (Caliper Life Sciences, Inc., Hopkinton, MA) without nitrogen gas stream; this usually took 30 min. The plate was washed three times with 300 μl of 6 M guanidine hydrochloride in 50 mM ammonium bicarbonate followed by washing with 3 $\times$ 300 μl of water. When on-bead methyl esterification was carried out (19), the beads were washed three times with 300 μl of 10 mM HCl, 50% aqueous acetonitrile, and acetonitrile successively. The well was incubated with 100 μl of 100 mM 3-methyl-1-*p*-tolyltriazene in dimethyl sulfoxide-ACN (1:1) for 60 min at 60 °C. The solution was removed by applying vacuum, and then the beads were washed with ACN, water, and MeOH (3 $\times$ 300 μl) successively. The hydrazone linkage between the oligosaccharide and the fluorescent probe on the bead was stabilized by incubation with a reducing reagent, 0.8 M borane-pyridine, according to the method reported previously (16). The reduction was performed at room temperature for 30 min in the dark. After the removal of the reaction mixture, the beads were washed with MeOH, ACN, and water (3 $\times$ 300 μl) successively. To the well 50 μl of 50 mM DTT in 5 mM ammonium bicarbonate was added, and the plate was incubated for 5 min at 60 °C and an additional 15 min at room temperature. The enriched *N*-glycans processed as above were recovered from the beads in the DTT solution.

Mass Spectrometry

The recovered *N*-glycans in the DTT solution (0.5 μl) were directly deposited on a target plate (AnchorChip 400/384, Bruker Daltonics, Bremen, Germany) mixed with an equivalent volume of the matrix solution, a 9:1 mixture of 2,5-dihydroxybenzoic acid and 2,5-dihydroxybenzoic acid sodium salt (10 mg/ml each in 30% ACN), and dried under vacuum to afford crystals of the analytes. The mass spectra were acquired with an UltraFlex II TOF/TOF instrument (Bruker Daltonics) in reflector, positive ion mode typically summing 500 shots.

Statistical Analysis

In this study, a maximum of 44 *N*-glycan peaks in MALDI-TOF MS spectra were picked using the software FlexAnalysis version 3 (Bruker Daltonics). All statistical analyses were performed using MATLAB (version 7.4, The Mathworks, Inc.) language with a Statistics Toolbox unless otherwise noted.

CDG Case—Each subtype was measured repeatedly ($n = 6$) because only one of each sample was available for the subtypes. The area of the isotopic peaks of each glycan was normalized to a known amount of internal standard (A2amide glycan). To identify *N*-glycans that can be used for the differentiation of type 1 CDG (CDG-I) subtypes and normal control, we performed a classification using an expectation maximization algorithm that separates a mixture of different data distributions in iterative steps of maximum likelihood estimation (30). Principal component analysis (PCA) was performed using Spotfire DecisionSite (version 9.0, Somerville, MA), and we plotted the first two principal components.

Hepatocellular Carcinoma (HCC) Case—The cutoff line for the calculation was defined as 0.3% of total area. Student's *t* test was used to calculate the statistical difference of disease *versus* normal status. A difference was considered statistically significant if p was <0.001. To identify the essential features to optimally classify the sera between the two states (disease and normal) we applied a sequential forward selection algorithm that sequentially selected a better combination of *N*-glycan peaks based on leave-one-out error rates of a k-nearest neighbor classifier ($k = 3$).

RESULTS

Rationale of BlotGlycoABC-based Clinical Glycomics—The new method described herein could provide an extremely facile and convenient approach for the enrichment analysis of complex glycoconjugates without any specialized training (Fig. 1*a*). To establish an all-in-one protocol, we designed a multifunctional molecular probe, *N*-(2-aminobenzoyl)cysteine hydrazide (ABCh), and used it for the conjugation with thiopropyl-Sepharose 6B to afford stable hydrazide-functionalized polymer support, namely the BlotGlycoABC bead (Fig.

[1] The abbreviations used are: PNGase F, peptide-*N*-glycosidase F; CDG, congenital disorders of glycosylation; HCC, hepatocellular carcinoma; PCA, principal component analysis; ABCh, *N*-(2-aminobenzoyl)cysteine hydrazide; CDG-I, type 1 CDG; CDG-II, type 2 CDG; PrEC, prostate epithelial cell.

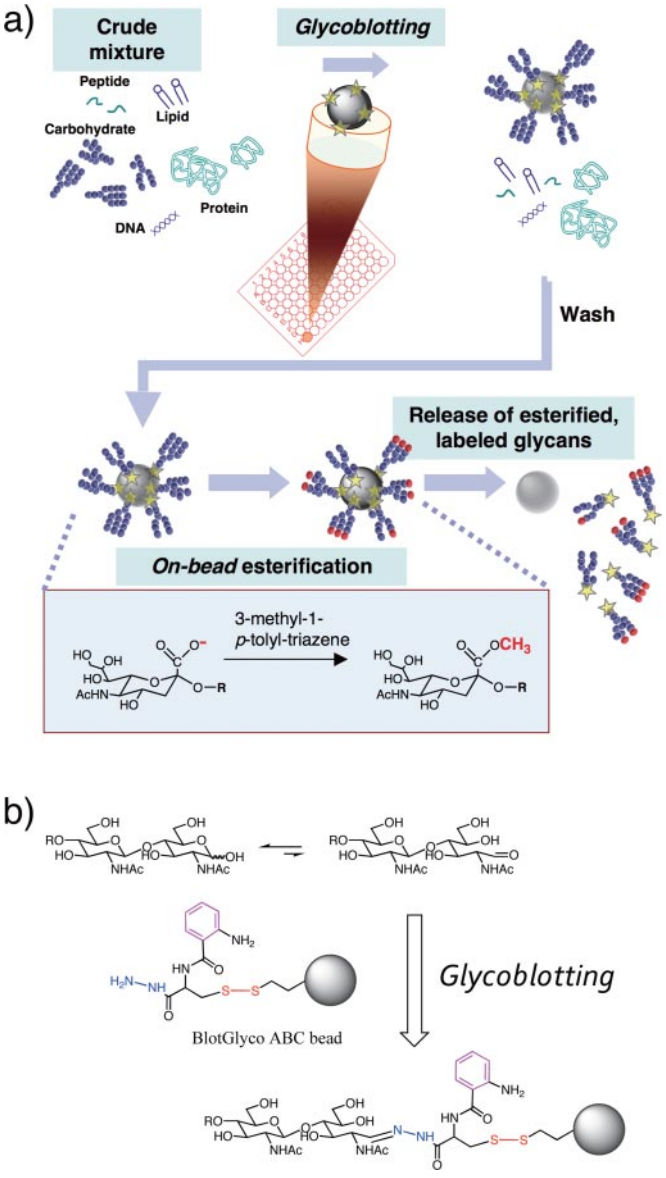

FIG. 1. **General protocol for an integrated glycoblotting technique.** *a*, a workflow of glycoblotting-based high throughput clinical glycomics. The steps included are: 1) chemoselective capturing of reducing sugars onto a hydrazide-functionalized bead using glycoblotting technology (15), 2) washing to remove any impurities, 3) on-bead methyl esterification of sialic acid residues followed by reduction of hydrazone linkage, and 4) recovery of modified *N*-glycans by reduction of the disulfide bond. *b*, glycoblotting by means of BlotGlycoABC. The chemical structure of the probe, ABCh, is shown; for the synthesis, see the supplemental note.

1*b*, the supplemental note, and supplemental Scheme 1). The hydrazide group reacts with aldehyde or ketone groups that are very rare in common biological samples except carbohydrates having a reducing hemiacetal terminus. Formation of the hydrazone bond between the BlotGlycoABC bead and glycans is reversible so that parental reducing sugars can be released; otherwise it could be reduced for conversion to a stable C–N bond (16). This chemistry is suitable to enrich carbohydrates from complex biological materials even in the presence of various amines and reagents used in proteomics sample preparation that contain a variety of reagents such as DTT, iodoacetamide, detergents, etc. Our method yielded quantitative ligation of general *N*-linked type oligosaccharides without any loss of sialic acids. The disulfide bond connecting thiopropyl-Sepharose 6B with the ABCh probe allowed quantitative recovery of enriched *N*-glycans by treatment with DTT in an elution buffer. The recovered samples containing neutral and acidic carbohydrates were then ready for the following quantitative analysis using HPLC and some of the MS analysis applications.

Although the intact neutral and sialylated glycans are recovered by the above procedure, sialylated oligosaccharides are known to decompose under general MS analysis due to their negative charges. Because stabilization of sialic acids is essential for the quantitative MS analysis of sialyloligosaccharides, a convenient *O*-methyl esterification of sialic acid residues by 3-methyl-1-*p*-tolyltriazene was incorporated into the protocol (19). Upon capturing total *N*-glycans via stable hydrazone linkage by means of the BlotGlycoABC bead, on-bead methyl esterification of sialic acids and on-bead reduction of the hydrazone bond were carried out to permit reliable/reproducible mass measurements for both neutral and acidic glycoforms under positive reflector mode in MALDI-TOF.

To illustrate the new method, human serum (2.5 μl) was subjected to the optimized protocol using the BlotGlycoABC bead. An aliquot of the "ready-to-analyze" sample solution equivalent to 25 nl of serum was directly deposited on a target plate and subjected to the MALDI-TOF analysis (positive reflector mode). We quantified 44 *N*-glycans (Fig. 2*a* and Table I) that were detectable in all samples and normalized their abundance to peak number 33 (spiked A2amide) as an internal standard. Once *N*-glycans are available by PNGase F treatment (20) of whole serum glycoproteins, it takes less than 4 h to identify gross *N*-glycan profiles with a routine operation using the BlotGlycoABC bead and MALDI-TOF MS. It should be noted that this solid-phase protocol is the first example of all-in-one glycoblotting technique in a single automatable workflow. We are currently investigating and developing a sample processing machine suited for the automated glycoblotting using BlotGlycoABC. In fact, the all-in-one glycoblotting protocol based on BlotGlycoABC could be preliminarily transferred to an automation platform by combined use with a standard multiwell filter plate format under a flow diagram optimized for the human serum application (supplemental Fig. 1). The validity of the automated protocol was assessed by simultaneous run of the same human serum digests (supplemental Fig. 2), and its accurate reliability was confirmed by good reproducibility (supplemental Table 2).

Detection of Alterations in CDG—Detection and profiling of *N*-glycans in whole serum glycoproteins is greatly beneficial for the rapid identification of abnormal protein glycosylation caused by congenital and acquired alteration. We tested our

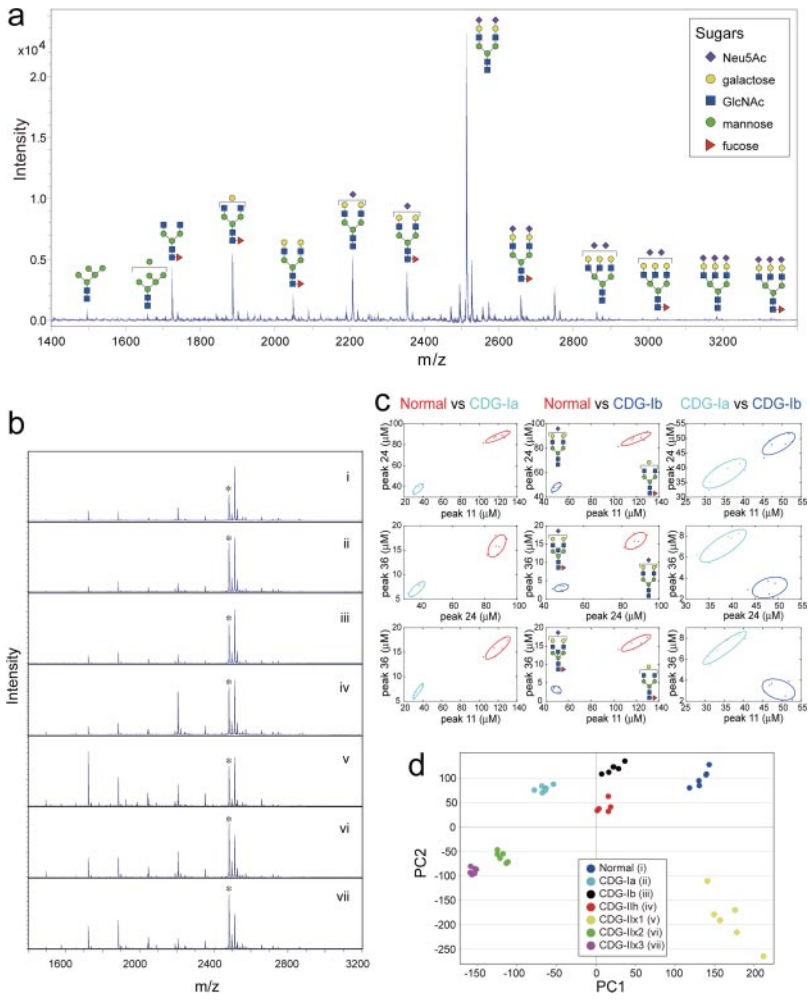

FIG. 2. **Profiling human serum glycoform.** *a*, MALDI-TOF MS spectrum of representative normal human serum *N*-glycans. Serum digested with trypsin and PNGase F was directly subjected to the protocol for *N*-glycan enrichment and derivatization using BlotGlycoABC. Note that sialyl *N*-glycans processed with on-bead methyl esterification were stabilized from desialylation so that quantitative glycomics analysis of total *N*-glycans is available. *b*, serum *N*-glycan profiles of CDG patients revealed by MALDI-TOF MS. *i*, healthy donor; *ii*, CDG-Ia; *iii*, CDG-Ib; *iv*, CDG-IIh; *v*, CDG-IIx1; *vi*, CDG-IIx2; *vii*, CDG-IIx3. The *asterisk* indicates a given amount of internal standard, A2amide. *c*, separation of CDG-I patients using an expectation maximization algorithm. A set of concentrations of the selected *N*-glycans can be used for the differentiation between healthy and CDG-I patients (*left* and *middle panels*). Similarly CDG-Ia and CDG-Ib can be successfully discriminated using the same set of *N*-glycans. *d*, PCA of all seven species of sera examined in this study for the CDG case. The first (*PC1*) and second (*PC2*) principal components were plotted, and the two components account for 41 and 37% of the variance, respectively.

technology on sera from patients suffering from the rare disease CDG, a group of inherited human disorders characterized by alterations in protein glycosylation (21). To date, more than 19 subtypes of CDG have been identified (22). They result from deficiencies in either the biosynthesis of *N*-glycan precursors or certain steps of *N*-glycan assembly, causing the elimination (type 1 CDG) or immature processing (type 2 CDG) of protein-bound sugar chains. With our glycoblotting technique based on BlotGlycoABC and MALDI-TOF MS, we could detect abnormal glycosylation patterns in the whole serum glycoproteins from the patients. Each analysis was repeated six times ($n = 6$), and the peak areas in the MALDI-TOF MS spectra were normalized to a given amount of internal standard, A2amide. As expected, for type 2 CDG (CDG-II) patients who experience a deficiency in a specific step(s) of glycosylation, we observed abnormal *N*-glycan profiles such as an increase of some immature small *N*-glycan chains (Fig. 2*b*, *iv–vii*) (CDG-IIx, unclassified subtype of CDG-II). On the other hand, *N*-glycans enriched from the CDG-I patient sera exhibited *N*-glycan profiles quite similar to the normal subject (Fig. 2*b*, *ii* and *iii*). However, the result also indicated a significant decrease of the total *N*-glycans (575 ± 46 and 692 ± 41 μM for CDG-Ia and CDG-Ib patients, respectively; see also supplemental Table 2) compared with that of normal donor (1011 ± 69 μM), clearly suggesting that the deficiency in CDG-I results in loss of whole glycan chains to some extent due to the failure in precursor biosynthesis.

The merit of using quantitative glycomics to discover diagnostic markers of CDG-I patients is evident because the data distributions formed by the abundance of the 42 *N*-glycans detected can be used for the facile differentiation of patients from normal serum (Fig. 2*c*, *left* and *middle panels*). The results also revealed that a couple of combinations of *N*-glycan abundance have been shown to prove a diagnostic differentiation between CDG-I patients CDG-Ia and CDG-Ib (Fig. 2*c*, *right panels*). In addition, we used PCA of acquired total *N*-glycan profiles to interpret the complex, multispectral dataset of all the CDG subtypes. The first two principal components clearly separated the CDG subtypes including normal donor. Theses results confirmed that the profile of the whole serum *N*-glycan set could clearly distinguish a certain subtype of CDG from the other subtype of CDG as well from healthy control.

Diagnostic Discrimination of Hepatocellular Carcinoma—To demonstrate the versatility of the present protocol in large

TABLE I

44 N-glycans derived from human serum were targeted in this study

Peak 33 is an internal standard spiked for the quantification. Compositional annotation and putative structures shown in abbreviation were achieved using GlycoSuite on-line database (Proteome Systems). Hex, hexose; HexNAc, *N*-acetylhexosamine; dHex, deoxyhexose.

Peak no.	*m/z*	Composition	Abbreviation
1	1495.511	Hex_2 + Man_3 $(GlcNAc)_2$	Man5
2	1520.543	$(HexNAc)_1$ $dHex_1$ + Man_3 $(GlcNAc)_2$	CoreFGN1
3	1536.538	Hex_1 $(HexNAc)_1$ + Man_3 $(GlcNAc)_2$	CoreG1GN1
4	1577.565	$(HexNAc)_2$ + Man_3 $(GlcNAc)_2$	NA2G0
5	1657.564	Hex_3 + Man_3 $(GlcNAc)_2$	Man6
6	1723.623	$(HexNAc)_2$ $dHex_1$ + Man_3 $(GlcNAc)_2$	NA2FG0
7	1739.617	Hex_1 $(HexNAc)_2$ + Man_3 $(GlcNAc)_2$	NA2G1
8	1780.644	$(HexNAc)_3$ + Man_3 $(GlcNAc)_2$	bisG0
9	1819.617	Hex_4 + Man_3 $(GlcNAc)_2$	Man7
10	1841.649	Hex_1 $(HexNAc)_1$ $(NeuAc)_1$ + Man_3 $(GlcNAc)_2$	A1(G1GN1)
11	1885.675	Hex_1 $(HexNAc)_2$ $dHex_1$ + Man_3 $(GlcNAc)_2$	NA2FG1
12	1901.670	Hex_2 $(HexNAc)_2$ + Man_3 $(GlcNAc)_2$	NA2
13	1926.702	$(HexNAc)_3$ $dHex_1$ + Man_3 $(GlcNAc)_2$	bisFG0
14	1942.697	Hex_1 $(HexNAc)_3$ + Man_3 $(GlcNAc)_2$	bis(G1)
15	1981.670	Hex_5 + Man_3 $(GlcNAc)_2$	Man8
16	1987.707	Hex_1 $(HexNAc)_1$ $dHex_1$ $(NeuAc)_1$ + Man_3 $(GlcNAc)_2$	A1F(G1GN1)
17	2003.702	Hex_2 $(HexNAc)_1$ $(NeuAc)_1$ + Man_3 $(GlcNAc)_2$	A1M1(G1GN1)
18	2044.729	Hex_1 $(HexNAc)_2$ $(NeuAc)_1$ + Man_3 $(GlcNAc)_2$	A1(G1)
19	2047.728	Hex_2 $(HexNAc)_2$ $dHex_1$ + Man_3 $(GlcNAc)_2$	NA2F
20	2088.755	Hex_1 $(HexNAc)_3$ $dHex_1$ + Man_3 $(GlcNAc)_2$	bisF(G1)
21	2104.750	Hex_2 $(HexNAc)_3$ + Man_3 $(GlcNAc)_2$	bis(G2)
22	2143.723	Hex_6 + Man_3 $(GlcNAc)_2$	Man9
23	2165.755	Hex_3 $(HexNAc)_1$ $(NeuAc)_1$ + Man_3 $(GlcNAc)_2$	A1Man5
24	2206.781	Hex_2 $(HexNAc)_2$ $(NeuAc)_1$ + Man_3 $(GlcNAc)_2$	A1
25	2247.808	Hex_1 $(HexNAc)_3$ $(NeuAc)_1$ + Man_3 $(GlcNAc)_2$	NA3(G1A1)
26	2250.808	Hex_2 $(HexNAc)_3$ $dHex_1$ + Man_3 $(GlcNAc)_2$	bisF(G2)
27	2266.802	Hex_3 $(HexNAc)_3$ + Man_3 $(GlcNAc)_2$	NA3
28	2352.839	Hex_2 $(HexNAc)_2$ $dHex_1$ $(NeuAc)_1$ + Man_3 $(GlcNAc)_2$	A1F
29	2393.866	Hex_1 $(HexNAc)_3$ $dHex_1$ $(NeuAc)_1$ + Man_3 $(GlcNAc)_2$	NA3F(G1A1)
30	2409.861	Hex_2 $(HexNAc)_3$ $(NeuAc)_1$ + Man_3 $(GlcNAc)_2$	bis(G2A1)
31	2412.860	Hex_3 $(HexNAc)_3$ $dHex_1$ + Man_3 $(GlcNAc)_2$	bisF(G3)
32	2469.882	Hex_3 $(HexNAc)_4$ + Man_3 $(GlcNAc)_2$	NA4(G3)/NA3bis
33	2481.893	Hex_2 $(HexNAcAmide)_2$ + Man_3 $(GlcNAc)_2$	A2amide
34	2511.892	Hex_2 $(HexNAc)_2$ $(NeuAc)_2$ + Man_3 $(GlcNAc)_2$	A2
35	2539.924	Hex_1 $(HexNAc)_3$ $dHex_2$ $(NeuAc)_1$ + Man_3 $(GlcNAc)_2$	
36	2555.919	Hex_2 $(HexNAc)_3$ $dHex_1$ $(NeuAc)_1$ + Man_3 $(GlcNAc)_2$	bisF(G2A1)
37	2571.914	Hex_3 $(HexNAc)_3$ $(NeuAc)_1$ + Man_3 $(GlcNAc)_2$	NA3(A1)
38	2615.940	Hex_3 $(HexNAc)_4$ $dHex_1$ + Man_3 $(GlcNAc)_2$	NA3Fbis
39	2631.935	Hex_4 $(HexNAc)_4$ + Man_3 $(GlcNAc)_2$	NA4
40	2657.950	Hex_2 $(HexNAc)_2$ $dHex_1$ $(NeuAc)_2$ + Man_3 $(GlcNAc)_2$	A2F
41	2717.971	Hex_3 $(HexNAc)_3$ $dHex_1$ $(NeuAc)_1$ + Man_3 $(GlcNAc)_2$	NA3F(A1)
42	2861.030	Hex_2 $(HexNAc)_3$ $dHex_1$ $(NeuAc)_2$ + Man_3 $(GlcNAc)_2$	bisF(A2)
43	2877.025	Hex_3 $(HexNAc)_3$ $(NeuAc)_2$ + Man_3 $(GlcNAc)_2$	NA3(A2)
44	3023.083	Hex_3 $(HexNAc)_3$ $dHex_1$ $(NeuAc)_2$ + Man_3 $(GlcNAc)_2$	NA3F(A2)
45	3182.136	Hex_3 $(HexNAc)_3$ $(NeuAc)_3$ + Man_3 $(GlcNAc)_2$	A3

scale clinical glycomics, we applied our technique to sera from multiple patients suffering from HCC. As anticipated, use of the glycoblotting protocol based on BlotGlycoABC and MALDI-TOF analysis allowed for rapid and quantitative *N*-glycan profiling of 103 human serum samples (83 patients and 20 normal donors). To identify the essential features to optimally classify the sera between the two relevant classes, disease and normal, we applied a sequential forward selection algorithm that sequentially selected a better combination of *N*-glycan peaks based on leave-one-out error rates of a *k*-nearest neighbor classifier ($k = 3$) (Fig. 3, *a* and *b*). When we chose the ratios of every two peaks among the acquired peaks that showed significant difference (two-sided *t* test, $p < 0.001$) between disease and control, the algorithm finally selected three features (ratios of *N*-glycan abundance; Fig. 3*c*) that distinguished HCC samples from normal controls with 100% accuracy (Fig. 3*a*). Thus, BlotGlycoABC-based whole serum *N*-glycan profiling was demonstrated to provide a con-

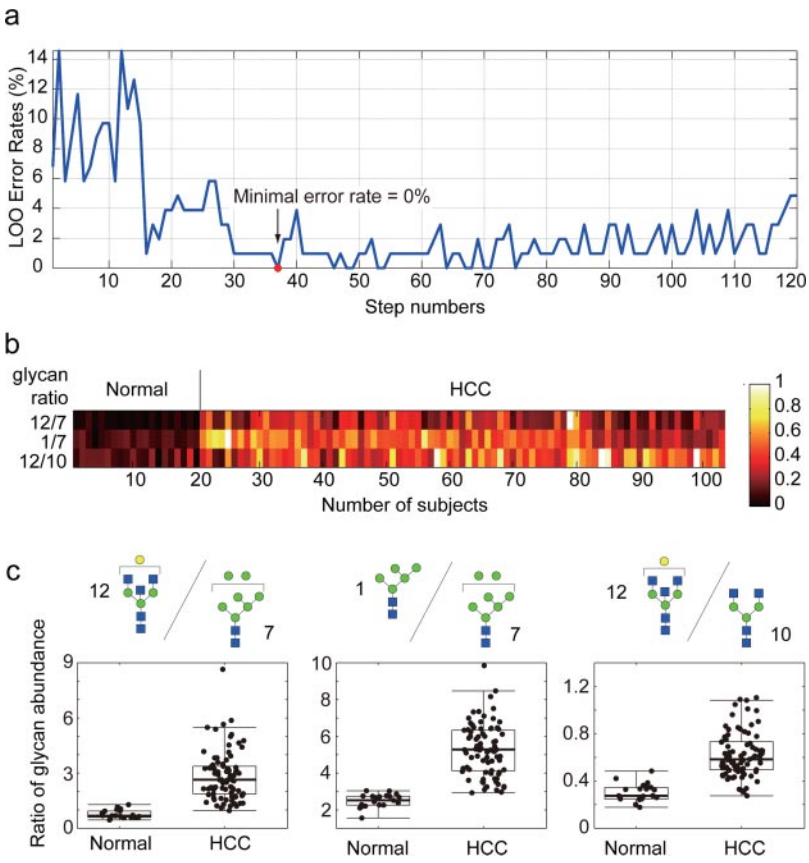

FIG. 3. **Classification by *N*-glycans derived from sera of hepatocellular carcinoma and normal control.** *a*, process of feature-subset selection in which sequential addition of the most significant *N*-glycans ratios at each step, testing a total of 276 models, resulted in a minimal error rate of 0%. *b*, heat map view of the selected three *N*-glycans ratios as features for the classification (*brighter color* indicates higher glycan abundance ratio). *c*, box plot expression of the selected features (ratios of *N*-glycan abundance, oligosaccharide structures, and peak numbers are shown in the figure). *LOO*, leave-one-out.

venient, noninvasive diagnostic tool for diseases that have previously been difficult to diagnose early or to differentiate.

Application to Cellular Glycomics—Besides serum, cells and tissues are also important biomaterials in clinical glycomics. We applied the enrichment protocol established above to cultured cells to investigate total cellular *N*-glycoforms. Human prostate cancer PC-3 cells and normal human prostate epithelial cells (PrECs) were cultured, and whole protein extracts were subjected to BlotGlycoABC bead processing. Like serum *N*-glycan profiles, total cellular glycomes were clarified with a small amount of starting material (5–8 $\times$ 10^6 cells), although we have not assessed the glycan profiles using other methods. The results showed that *N*-glycan profiles unique for each cell lines were successfully detected and that our approach described above for serum glycomics is equally well suited to cellular glycomics (Fig. 4). The optimization of cellular/tissue glycomics is currently under examination to make the general protocol amenable for further high throughput features.

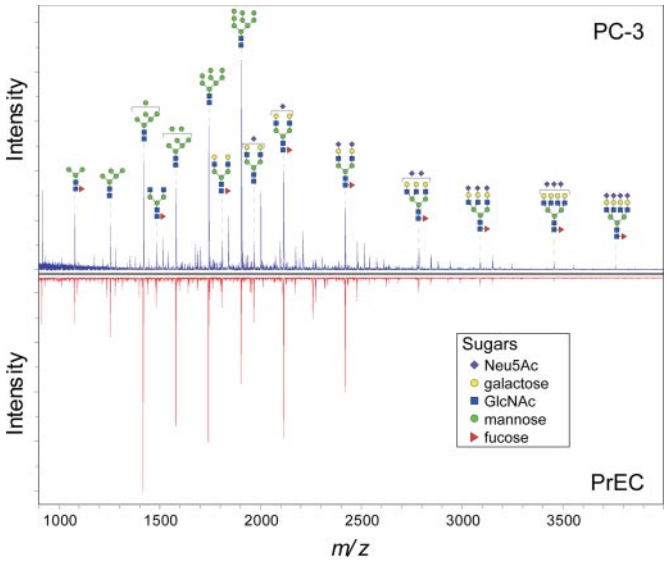

FIG. 4. **Total cellular glycomes of human prostate cancer PC-3 cells and normal human PrECs.** Cells grown in a 10-cm dish were subjected to the glycoblotting protocol using BlotGlycoABC and MS analysis (also see the supplemental note).

DISCUSSION

A growing number of studies that demonstrate alterations in protein glycosylation with disease states have been reported (23–26). Our results show the potential clinical value of quantitative analysis of whole serum *N*-glycan profiles acquired with MALDI-TOF MS. Recently the usefulness of MALDI-TOF MS for the profiling of *N*-glycans in serum has been anticipated in both quantitative and qualitative analysis (27, 28) to facilitate the detection of clinically relevant tumors. Our method would append unparalleled feasibility of glycan en-

richment and derivatization for the quantitative and high throughput MS analysis in clinical assessment. The truly total *N*-glycomics analyses were made possible by incorporation of the integrated glycoblotting bead, BlotGlycoABC, introduced herein and on-bead methyl esterification. The present protocol requires only a 2.5-μl aliquot of human whole serum, and the multistep processes for the derivatization were successfully performed on a solid phase in a single sweep 4-h run including MALDI-TOF MS, thereby dramatically improving the efficiency and time of operation. Because of meaningful improvements demonstrated in serum glycan preparation and analysis, our protocol could also be used for glycan enrichment analysis from cellular samples. We demonstrated preliminarily that the total cellular *N*-glycomes of human prostate cancer PC-3 cells and their normal counterpart cells grown in a single 10-cm dish were revealed with glycoblotting using BlotGlycoABC and MALDI-TOF MS analysis. The methods for cellular glycome profiling were essentially the same as those for serum except for the minor modification in sample pretreatment (Fig. 4 and see the supplemental note). The results clearly indicated a significant difference in the *N*-glycan structures between PC-3 cells and normal PrECs in pattern and quantity of glycans. We believe that glycomics at the cellular and tissue level would be greatly facilitated by using our approach.

Recent findings on defects that underlie each CDG have revealed that glycan analysis seems to be insufficient to pinpoint the defect in some CDG-II (29, 30). However, our results clearly demonstrated that the dataset of *N*-glycan abundance in each subtype patient was evidently segregated in expression space upon principal component analysis, although we could not test multiple sera for each subtype. Thus, for CDG, discovery of the rare case would be more imperative through quantitative glycomics at common screening tests such as the newborn screening program because CDG along with other diseases can be detected by a simple blood test, and we believe that our glycoblotting technique could be the approach to use because of its reproducibility and ease of use. It would also be interesting to apply the technique to other diseases that have been characterized with altered glycosylation in transferrin, such as congenital galactosemia and chronic alcohol intake, to reveal the validity of the analysis performed in this study.

Based on the *N*-glycan profiling by large scale glycomics of HCC samples (83 patients and 20 normal donors), the statistical approach allowed identification of a set of specific *N*-glycan expression ratios that is optimal for pattern classification. We differentiated HCC samples from normal controls with 100% accuracy by means of the above specific *N*-glycan profiles. Therefore, the quantitative profile of selected glycoforms would have potential clinical information as a novel and efficient diagnostic biomarker for human HCC, although the information obtained here should be tested using other clinical variables and correlation with medical facts of hepatitis B virus and/or hepatitis C virus infection.

Reproducible mass spectra were obtained throughout the MALDI-TOF MS analysis because of quantitative methyl esterification of sialic acid residues, which made the method amenable to simultaneous and quantitative profiling of neutral and acidic *N*-glycans. Despite such advantages over other analytical methods, we had to pay attention to the fact that the intensity of mass signals often depends upon the individual MALDI equipment used during the analysis of the wide molecular weight range of *N*-glycans as well as chemical structures of the tagging group selected (supplemental Fig. 3 and supplemental Table 3). It is likely that laser source applied in each MALDI system affects significantly ionization efficiency of certain molecules such as high molecular weight glycans with multiple sialic acid residues. Comparing the present results (supplemental Table 1) with our previous data (20), the quantity of the fully sialylated triantennary glycans was estimated to be lower than that of the previous study. This result may be caused by a difference in chemical structures between the peptide-based high sensitivity tag (20, 31) and the present probe designated in BlotGlycoABC as well as a difference in the laser power and wavelength used in each measurement (32). To achieve much more accurate and reliable quantitative analysis in MALDI mass-based glycomics, we may need to develop a new type of molecular probes that provides such high molecular weight glycans with much higher ionization efficiency.

We believe that the integrated glycoblotting technique utilizing BlotGlycoABC would greatly facilitate discovery research for new biomarkers of various diseases using multiple serum and cellular samples. Because the chemistry used for solid-phase manipulation of the enriched *N*-glycans is well suited for the derivatization required in conventional HPLC, LC-MS, and/or DNA sequencer-based analysis, the recovered *N*-glycans tagged with optimized chemical probes can be used for these analytical methods.

Acknowledgments—We thank Dr. H. H. Freeze for providing sera of CDG patients and valuable advice and K. Hirose, Hokkaido University, for assistance with statistical analysis. We also thank A. Yamauchi, Hokkaido University, for technical assistance.

* This work was supported in part by a grant for "Development of Systems and Technology for Advanced Measurement and Analysis (SENTAN)" from the Japan Science and Technology Agency (JST) and Grant-in-aid 17205015 from the Ministry of Education, Culture, Science, and Technology, Japan. The costs of publication of this article were defrayed in part by the payment of page charges. This article must therefore be hereby marked "*advertisement*" in accordance with 18 U.S.C. Section 1734 solely to indicate this fact.

[S] The on-line version of this article (available at http://www.mcponline.org) contains supplemental material.

** To whom correspondence should be addressed: Laboratory of Advanced Chemical Biology, Graduate School of Life Science, Frontier Research Center for Post-Genomic Science and Technology, Hokkaido University, Sapporo 001-0021, Japan. Tel.: 81-11-706-9043; Fax: 81-11-706-9042; E-mail: shin@glyco.sci.hokudai.ac.jp.

REFERENCES

1. Hakomori, S. (2001) Tumor-associated carbohydrate antigens defining tumor malignancy: basis for development of anti-cancer vaccines. *Adv. Exp. Med. Biol.* **491,** 369–402
2. Zaia, J. (2004) Mass spectrometry of oligosaccharides. *Mass Spectrom. Rev.* **23,** 161–227
3. Dell, A., and Morris, H. R. (2001) Glycoprotein structure determination by mass spectrometry. *Science* **291,** 2351–2356
4. Kurogochi, M., and Nishimura, S.-I. (2004) Structural characterization of N-glycopeptides by matrix-dependent selective fragmentation of MALDI-TOF/TOF tandem mass spectrometry. *Anal. Chem.* **76,** 6097–6101
5. Takegawa, Y., Deguchi, K., Ito, S., Yoshioka, S., Nakagawa, H., and Nishimura, S.-I. (2005) Simultaneous analysis of 2-aminopyridine-derivatized neutral and sialylated oligosaccharides from human serum in the negative-ion mode by sonic spray ionization ion trap mass spectrometry. *Anal. Chem.* **77,** 2097–2106
6. Kirmiz, C., Li, B., An, H. J., Clowers, B. H., Chew, H. K., Lam, K. S., Ferrige, A., Alecio, R., Borowsky, A. D., Sulaimon, S., Lebrilla, C. B., and Miyamoto, S. (2007) A serum glycomics approach to breast cancer biomarkers. *Mol. Cell. Proteomics* **6,** 43–55
7. Neville, D. C., Coquard, V., Priestman, D. A., te Vruchte, D. J., Sillence, D. J., Dwek, R. A., Platt, F. M., and Butters, T. D. (2004) Analysis of fluorescently labeled glycosphingolipid-derived oligosaccharides following ceramide glycanase digestion and anthranilic acid labeling. *Anal. Biochem.* **331,** 275–282
8. Tomiya, N., Kurono, M., Ishihara, H., Tejima, S., Endo, S., Arata, Y., and Takahashi, N. (1987) Structural analysis of N-linked oligosaccharides by a combination of glycopeptidase, exoglycosidases, and high-performance liquid chromatography. *Anal. Biochem.* **163,** 489–499
9. Powell, A. K., and Harvey, D. J. (1996) Stabilization of sialic acids in N-linked oligosaccharides and gangliosides for analysis by positive ion matrix-assisted laser desorption/ionization mass spectrometry. *Rapid Commun. Mass Spectrom.* **10,** 1027–1032
10. Sekiya, S., Wada, Y., and Tanaka, K. (2005) Derivatization for stabilizing sialic acids in MALDI-MS. *Anal. Chem.* **77,** 4962–4968
11. Mechref, Y., Kang, P., and Novotny, M. V. (2006) Differentiating structural isomers of sialylated glycans by matrix-assisted laser desorption/ionization time-of-flight/time-of-flight tandem mass spectrometry. *Rapid Commun. Mass Spectrom.* **20,** 1381–1389
12. Callewaert, N., Van Vlierberghe, H., Van Hecke, A., Laroy, W., Delanghe, J., and Contreras, R. (2004) Noninvasive diagnosis of liver cirrhosis using DNA sequencer-based total serum protein glycomics. *Nat. Med.* **10,** 429–434
13. Laroy, W., Contreras, R., and Callewaert, N. (2006) Glycome mapping on DNA sequencing equipment. *Nat. Protoc.* **1,** 397–405
14. Morelle, W., Canis, K., Chirat, F., Faid, V., and Michalski, J. C. (2006) The use of mass spectrometry for the proteomic analysis of glycosylation. *Proteomics* **6,** 3993–4015
15. Nishimura, S.-I., Niikura, K., Kurogochi, M., Matsushita, T., Fumoto, M., Hinou, H., Kamitani, R., Nakagawa, H., Deguchi, K., Miura, N., Monde, K., and Kondo, H. (2005) High-throughput protein glycomics: combined use of chemoselective glycoblotting and MALDI-TOF/TOF mass spectrometry. *Angew. Chem. Int. Ed. Engl.* **44,** 91–96
16. Lohse, A., Martins, R., Jorgensen, M. R., and Hindsgaul, O. (2006) Solid-phase oligosaccharide tagging (SPOT): Validation on glycolipid-derived structures. *Angew. Chem. Int. Ed. Engl.* **45,** 4167–4172
17. Niikura, K., Kamitani, R., Kurogochi, M., Uematsu, R., Shinohara, Y., Nakagawa, H., Deguchi, K., Monde, K., Kondo, H., and Nishimura, S.-I. (2005) Versatile glycoblotting nanoparticles for high-throughput protein glycomics. *Chem. Eur. J.* **11,** 3825–3834
18. Shimaoka, H., Kuramoto, H., Furukawa, J., Miura, Y., Kurogochi, M., Kita, Y., Hinou, H., Shinohara, Y., and Nishimura, S.-I. (2007) One-pot solid-phase glycoblotting and probing by transoximization for high-throughput glycomics and glycoproteomics. *Chem. Eur. J.* **13,** 1664–1673
19. Miura, Y., Shinohara, Y., Furukawa, J. I., Nagahori, N., and Nishimura, S.-I. (2007) Rapid and simple solid-phase esterification of sialic acid residues for quantitative glycomics by mass spectrometry. *Chem. Eur. J.* **13,** 4797–4804
20. Kita, Y., Miura, Y., Furukawa, J. I., Nakano, M., Shinohara, Y., Ohno, M., Takimoto, A., and Nishimura, S.-I. (2007) Quantitative glycomics of human whole serum glycoproteins based on the standardized protocol for liberating N-glycans. *Mol. Cell. Proteomics* **6,** 1437–1445
21. Mandato, C., Brive, L., Miura, Y., Davis, J. A., Di Cosmo, N., Lucariello, S., Pagliardini, S., Seo, N. S., Parenti, G., Vecchione, R., Freeze, H. H., and Vajro, P. (2006) Cryptogenic liver disease in four children: a novel congenital disorder of glycosylation. *Pediatr. Res.* **59,** 293–298
22. Freeze, H. H., and Aebi, M. (2005) Altered glycan structures: the molecular basis of congenital disorders of glycosylation. *Curr. Opin. Struct. Biol.* **15,** 490–498
23. Baldus, S. E., Wienand, J. R., Werner, J. P., Landsberg, S., Drebber, U., Hanisch, F. G., and Dienes, H. P. (2005) Expression of MUC1, MUC2 and oligosaccharide epitopes in breast cancer: prognostic significance of a sialylated MUC1 epitope. *Int. J. Oncol.* **27,** 1289–1297
24. Comunale, M. A., Lowman, M., Long, R. E., Krakover, J., Philip, R., Seeholzer, S., Evans, A. A., Hann, H. W., Block, T. M., and Mehta, A. S. (2006) Proteomic analysis of serum associated fucosylated glycoproteins in the development of primary hepatocellular carcinoma. *J. Proteome Res.* **5,** 308–315
25. Dwek, M. V., Lacey, H. A., and Leathem, A. J. (1998) Breast cancer progression is associated with a reduction in the diversity of sialylated and neutral oligosaccharides. *Clin. Chim. Acta* **271,** 191–202
26. Kyselova, Z., Mechref, Y., Al Bataineh, M. M., Dobrolecki, L. E., Hickey, R. J., Vinson, J., Sweeney, C. J., and Novotny, M. V. (2007) Alterations in the serum glycome due to metastatic prostate cancer. *J. Proteome Res.* **6,** 1822–1832
27. Morelle, W., Flahaut, C., Michalski, J. C., Louvet, A., Mathurin, P., and Klein, A. (2006) Mass spectrometric approach for screening modifications of total serum N-glycome in human diseases: application to cirrhosis. *Glycobiology* **16,** 281–293
28. Kranz, C., Ng, B. G., Sun, L., Sharma, V., Eklund, E. A., Miura, Y., Ungar, D., Lupashin, V., Winkel, D. R., Cipollo, J. F., Costello, C. E., Loh, E., Hong, W., and Freeze, H. H. (2007) COG8 deficiency causes new Congenital Disorder of Glycosylation type IIh. *Hum. Mol. Genet.* **16,** 731–741
29. Wu, X., Steet, R. A., Bohorov, O., Bakker, J., Newell, J., Krieger, M., Spaapen, L., Kornfeld, S., and Freeze, H. H. (2004) Mutation of the COG complex subunit gene COG7 causes a lethal congenital disorder. *Nat. Med.* **10,** 518–523
30. Redner, R. A., and Walker, H. F. (1984) Mixture densities, maximum likelihood and the EM algorithm. *Soc. Ind. Appl. Math. Rev.* **26,** 195–239
31. Uematsu, R., Furukawa, J., Nakagawa, H., Shinohara, Y., Deguchi, K., Monde, K., and Nishimura, S.-I. (2005) High throughput quantitative glycomics and glycoform-focused proteomics of murine dermis and epidermis. *Mol. Cell. Proteomics* **4,** 1977–1989
32. Holle, A., Haase, A., Kayser, M., and Höhndorf, J. (2006) Optimizing UV laser focus profiles for improved MALDI performance. *J. Mass Spectrom.* **41,** 705–716